

# EMBEDDING FORMULAE FOR DIFFRACTION BY NON-PARALLEL SLITS

by E. A. Skelton<sup>1</sup>, R. V. Craster<sup>1</sup> & A. V. Shanin<sup>2</sup>

(<sup>1</sup> *Department of Mathematics, Imperial College of Science, Technology and Medicine, London SW7 2BZ, U.K.* <sup>2</sup> *Department of Physics (Acoustics Division), Moscow State University, 119992, Leninskie Gory, Moscow, Russia*)

[Received October 24, 2007]

## Summary

Embedding formulae for diffraction theory encode the diffraction coefficients for some given wave incidence on a scatterer in terms of the directivity from a single, or reduced number of, scattering problems. If one deduces the relation between these directivities then the resulting formulae enable rapid computations and allow one to concentrate computational resources accordingly. Unfortunately, the range of applicability of embedding formulae is currently rather restricted. In this article we demonstrate how embedding is applied to plane wave scattering by non-parallel strips or slits. Primarily we concentrate upon the problem of a line crack, or strip, inclined to a flat infinite surface and we derive and implement the embedding formula. Various other generalisations are possible given these formulae and we outline them.

## 1. Introduction

The diffraction of waves by a sharp corner or edge is a ubiquitous feature that arises in many guises for scattering problems in water waves (1), acoustics (2), electromagnetism (3) and elasticity (4) and wherever waves interact with real structures or obstacles.

The most important quantity required in any scattering calculation is the behaviour of the field far from the scatterer and this is, in an infinite medium, characterised by the so-called directivity which is a function of both incident and observation angles. In elasticity, directivities are associated with shear and compressional waves, and possibly surface or interfacial waves too. Given the importance of wave scattering and its many applications there has been considerable effort and progress made with solving the underlying equations numerically, asymptotically and exactly. If one has to proceed numerically then it can be time consuming to do a parametric study for, say, all incoming angles of incidence and any method that reduces this burden is welcome.

Fortunately there does exist a technique, little-used, that could revolutionise many scattering calculations: embedding formulae. Embedding formulae employ the philosophy that instead of actually solving the physical problem of interest and extracting the directivity directly one should instead only solve a small number of auxiliary problems. The directivity of the physical problem is then constructed from the directivities of these few auxiliary equations. The few auxiliary equations take comparatively little time to evaluate and so this is much more efficient. At first sight this seems too good to be true - and indeed there are some difficulties, primarily: what auxiliary problems do we choose? How exactly are they related to the physical problem?

Historically it appears that embedding formulae were introduced by Williams (5) for a two-dimensional problem in acoustics. This elegant analysis shows that for a finite straight rigid strip, or gap between rigid screens, the directivity for *all* incident angles can be obtained from that found for a plane wave incident at the grazing angle. This rather remarkable result triggered a couple of contemporaneous articles (6, 7) that used integral equation formulations to extend these ideas to impedance conditions or to elasticity. Several authors (1, 8, 9, 10, 11) then solved useful and interesting examples from water wave and acoustic theory using formulations and manipulations based upon integral equation theory. All of these articles, bar (9), require all of the scatterers to be thin parallel strips and the integral equations to have difference kernels. The article by Biggs and Porter (9) relaxes this and shows that for a particular sum and difference kernel progress can be similarly made. There are also interesting connections to the theory of integral equations themselves, (12), and as such embedding has wider application. As a result, one might then wonder whether embedding is limited to problems which must be formulated as an integral equation, or as a system of integral equations, and whether it is solely limited to parallel scatterers, any of which would seem to limit its wider applicability.

More recently, in (13) (hereafter [I]), it was shown that embedding formulae emerge naturally, and directly, from the governing equations independent of the solution procedure. Hence embedding formulae are not dependent upon there being an integral equation formulation. In [I], for scattering by parallel cracks and strips, it was shown that one could also extend the formulae in a number of different directions: to elasticity, to three dimensions (see also (14, 15)) and by utilizing asymptotic methods. The fundamental building block for the auxiliary solutions turns out to be an edge Green's function with, in 2D (3D), a line (point) source placed on the sharp edges. The terminology edge Green's function now seems to us more appropriate, or at least more recognisable, than the use of overly singular eigensolutions in [I], and so we now use the former. For straight and parallel cracks or strips the number of auxiliary solutions is equal, in the absence of any symmetries, to the number of edges in 2D. Nonetheless in [I] the theory is still for parallel scatterers, but that restriction has now been overcome. In (16) (hereafter [II]) embedding formulae for wedge and angular geometries (of rational angle) are derived using auxiliary solutions that are driven by multipoles. This allows scattering by angular shapes, such as an equilateral triangle, to become subsumed within the embedding technology. It is arguable that having auxiliary solutions that are highly singular at the edges is not computationally ideal, as numerical schemes are usually constructed explicitly to avoid singularities at edges, and (17) shows how this approach relates to auxiliary solutions composed of incoming plane waves. The typical scattering geometries covered in [I] and [II] are shown in figure 1(a, b).

We now surmount a further hurdle, that of problems that involve a straight strip (or strips) not parallel to a straight infinitely long surface (see figure 1c) or to each other. This is a confluence of two issues, the strip has an edge and the bounding surface is not parallel to it; we shall assume that it makes a rational angle with the strip. It turns out that this too can be subsumed within the current embedding technology by generalising ideas from [I] together with [II]; it is interesting to note that from an integral equation point of view, from which one could approach this problem, one has a sum and difference kernel. We shall however take the physical route of [I] and utilize auxiliary problems based upon edge Green's functions and demonstrate how embedding formulae emerge. Exact and numerical solutions are given to demonstrate their utility.

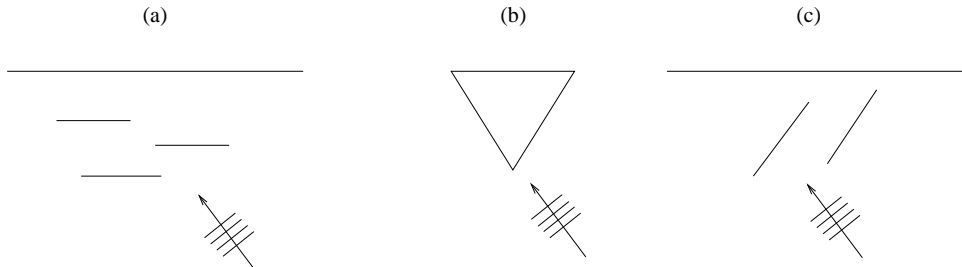


**Fig. 1** The generic types of geometry considered in [I] (a), in [II] (b) and here (c).

An outline of the article is as follows: The ideas are somewhat involved so we begin in section 2 by recapping the ideas of (13, 16) using scattering by a semi-infinite plate as a vehicle. In [I] this example was treated using a first-order operator, here we demonstrate that the scheme can also be developed using other higher-order operators (these are more singular than the original) to deduce many equivalent embedding formulae. The semi-infinite example is, in some ways harder than finite strips as it has a penumbral field and thus some of the technical steps, i.e. the application of an operator to this field are hard to formally justify. The explicit demonstration that the embedding formulae are true by construction is therefore in itself valuable. Indeed, at present, it is vital that the semi-infinite case be explicitly solved to ensure that the penumbral field actually plays no role, it is certainly unclear a-priori that applying an operator to that penumbral field and then manipulating the result does not contrive to create additional terms. Once the semi-infinite case has been proved correct one can, if we have, say, a half-plane and several finite strips, decompose the solution into a sum of half-plane and “compact” (purely finite) pieces, and prove the embedding formulae separately for the compact piece. Since there are no penumbral waves in the far field for this then it can be rigorously shown that the steps we use are formally correct.

We then use these ideas, and formulae, to tackle strips inclined to surfaces in section 3 and show how this relates to the linear superposition approach used in (17) in section 4. Clearly the whole idea is useless if it cannot be efficiently implemented numerically, we do so in section 5. The basic idea and operator actually allow an even wider class of problems to be tackled and we illustrate one (two perpendicular strips) example in detail in section 6, showing that coupled operators can be developed and used. Some concluding remarks are presented in section 7.

## 2. Embedding formulae for the Sommerfeld problem

The basic ideas of embedding are illustrated using a problem ubiquitous in diffraction theory, that of scattering by a semi-infinite half plane in 2D commonly called the Sommerfeld problem; the treatment of this using Wiener-Hopf theory is a standard example (1, 18) and the directivities form an integral part of the geometric theory of diffraction (19). Moreover, once illustrated on this relatively straightforward example the details of finite length, multiple scatterers and an inclined surface can all be readily incorporated.

### 2.1 Formulation

The Helmholtz equation

$$\nabla^2 u + k^2 u = 0, \quad (2.1)$$

is satisfied in the 2-dimensional infinite domain, described by Cartesian coordinates  $(x, y)$ , or cylindrical polar coordinates  $(r, \theta)$ . A semi-infinite planar crack occupies  $y = 0, x > 0$ , on which the Neumann boundary condition,  $\partial u / \partial y = 0$ , is required to hold.

The total field,  $u$  is the sum of an incident plane wave  $u^{in}$ ,

$$u^{in} = \exp[-ik(x \cos \theta^{in} + y \sin \theta^{in})] = \exp[-ikr \cos(\theta - \theta^{in})], \quad (2.2)$$

and a scattered field  $u^{sc}$ , which must satisfy a radiation condition as  $r \rightarrow \infty$ . Additionally, Meixner's edge condition that no energy is created at the edge of the crack must also be satisfied for physically meaningful solutions, together with the boundary condition on the crack surface. Hence as  $r \rightarrow 0$  the asymptotic behaviour of the total field must be of the form

$$u \sim K_1(\theta^{in}) r^{\frac{1}{2}} \cos\left(\frac{\theta}{2}\right), \quad (2.3)$$

This expression can be made more general, if required, via an eigenfunction expansion as briefly described in [II]

$$u \sim \sum_{j \text{ odd}} K_j(\theta^{in}) S_j, \quad (2.4)$$

with

$$S_j = B_j J_{j/2}(kr) \cos\left(\frac{j\theta}{2}\right), \quad B_j = \Gamma\left(\frac{j+2}{2}\right) \left(\frac{2}{k}\right)^{j/2}, \quad j = 1, 3, 5, \dots \quad (2.5)$$

where  $J_{j/2}$  is the Bessel function of the first kind of order  $j/2$  and  $\Gamma$  is the gamma function. This ensures that the asymptotic behaviour of  $S_j$  is

$$S_j \sim r^{j/2} (1 + O(r^2)) \cos\left(\frac{j\theta}{2}\right) \quad \text{as } r \rightarrow 0. \quad (2.6)$$

It is also convenient here to introduce some solutions of the Helmholtz equation (2.1) in the region  $r > 0$ , that satisfy the Neumann boundary condition on the crack surface, but whose behaviour near the crack tip is too singular to satisfy the Meixner condition (2.3) there:

$$\hat{u}_j = A_j H_{j/2}(kr) \cos\left(\frac{j\theta}{2}\right), \quad A_j = \frac{i\pi}{\Gamma(j/2)} \left(\frac{k}{2}\right)^{j/2}, \quad j = 1, 3, 5, \dots \quad (2.7)$$

where  $H_{j/2}$  is the Hankel function of order  $j/2$ . Thus, the asymptotic behaviour of these edge Green's functions is

$$\hat{u}_j \sim r^{-j/2} (1 + O(r^2)) \cos\left(\frac{j\theta}{2}\right) \quad \text{as } r \rightarrow 0. \quad (2.8)$$

These correspond physically to multipoles placed at the tip of the crack and as such these solutions are edge Green's functions (overly singular eigensolutions).

In the far-field, the scattered field comprises partial plane waves, as a result of geometrical

scattering effects due to the semi-infinite length of the scatterer, which are omitted from the following analysis for clarity of exposition, together with the modulated cylindrically spreading wave, which is of interest here. This has the form

$$u^{sc} \sim D(\theta, \theta^{in}) \frac{e^{i(kr - \pi/4)}}{(2\pi kr)^{\frac{1}{2}}}, \quad \text{as } r \rightarrow \infty, \quad (2.9)$$

and is characterised by the coefficient  $D(\theta, \theta^{in})$  which is the directivity of the field and is a function of both the angle of observation  $\theta$  and of the angle of incidence  $\theta^{in}$ . Similarly a directivity is deduced for the edge Green's functions, using

$$\hat{u}_j \sim \hat{D}_j(\theta) \frac{e^{i(kr - \pi/4)}}{(2\pi kr)^{\frac{1}{2}}}, \quad \text{as } r \rightarrow \infty, \quad (2.10)$$

and  $\hat{D}_j(\theta)$  is only a function of the observation angle. The aim is to be able to write  $D(\theta, \theta^{in})$  completely in terms of  $\hat{D}_j(\theta)$  and  $\hat{D}_j(\theta^{in})$ . For this problem, the directivities of the edge Green's functions are obtained directly from the large argument asymptotics of equation (2.7) as

$$\hat{D}_j(\theta) = \frac{2i\pi}{\Gamma(j/2)} \left( \frac{-ik}{2} \right)^{\frac{j}{2}} \cos\left(\frac{j\theta}{2}\right). \quad (2.11)$$

The solution method proceeds by applying Green's theorem for a source-free region to the pairs of functions  $u^{sc}$  and  $\hat{u}_j$ :

$$\int_C \left( \hat{u}_j \frac{\partial}{\partial n} u^{sc} - u^{sc} \frac{\partial}{\partial n} \hat{u}_j \right) ds = 0, \quad (2.12)$$

where  $\mathbf{n}$  is the outward normal to the contour. The contour  $C$  is the keyhole contour passing along the straight crack, enclosing the tip in a small circle and completed by a large circle that can be taken out to infinity (cf figure 2 without the inclined boundary).

The asymptotic expansions (2.4)–(2.8) allow the integral around the small circle to be evaluated as

$$\lim_{r \rightarrow 0} \int_0^{2\pi} \left( \hat{u}_j \frac{\partial}{\partial r} u^{sc} - u^{sc} \frac{\partial}{\partial r} \hat{u}_j \right) r d\theta = \pi j K_j(\theta_{in}), \quad (2.13)$$

whilst the far-field asymptotic expansions (2.9)–(2.11) show that the integral around the large circle is zero. Hence, from Green's theorem

$$\pi j K_j(\theta^{in}) = \int_{\mathcal{L}} \left( \hat{u}_j \frac{\partial}{\partial n} u^{sc} - u^{sc} \frac{\partial}{\partial n} \hat{u}_j \right) ds = - \int_{\mathcal{L}} \left( \hat{u}_j \frac{\partial}{\partial n} u^{in} - u^{in} \frac{\partial}{\partial n} \hat{u}_j \right) ds, \quad (2.14)$$

where  $\mathcal{L}$  is the straight portion of the contour along the crack surfaces, upon which  $\partial(u^{sc} + u^{in})/\partial n = 0$  and  $\partial \hat{u}_j/\partial n = 0$ . A similar application of Green's theorem to the pairs of functions  $u^{in}$  and  $\hat{u}_j$  results in the second integral of equation (2.14), together with an integral around the small circle, which is zero as  $r \rightarrow 0$ , and an integral around the large circle which can be evaluated using the far-field asymptotic expansion (2.10). Thus

$$-2i\hat{D}_j(\theta^{in}) = - \int_{\mathcal{L}} \left( \hat{u}_j \frac{\partial}{\partial n} u^{in} - u^{in} \frac{\partial}{\partial n} \hat{u}_j \right) ds = \pi j K_j(\theta^{in}). \quad (2.15)$$

This is a useful result from embedding whereby the near field of the physical problem is related to the far field of the edge Green's functions and is a restatement of the reciprocity principle.

## 2.2 First order operator embedding formula

An embedding formula was obtained in [I] by constructing a differential operator

$$H_1 = \frac{\partial}{\partial x} + ik \cos \theta^{in}, \quad (2.16)$$

and defining a new function  $\bar{u}_1$  as

$$\bar{u}_1 = H_1 u. \quad (2.17)$$

As noted in [I] the operator  $H_1$  has the following properties:

1. It maps any solution of the Helmholtz equation into another solution of the Helmholtz equation.
2. It maintains the Neumann boundary condition on the crack faces (and Dirichlet and impedance conditions if required).
3.  $H_1 u^{in} = 0$ .

Equations (2.4)–(2.6) for  $u$  and (2.8) for  $\hat{u}_j$  show that the asymptotic behaviour of  $\bar{u}_1$  near the tip is

$$\bar{u}_1 = H_1 u \sim \frac{K_1(\theta^{in})}{2r^{\frac{1}{2}}} \cos\left(\frac{\theta}{2}\right) + O(r^{\frac{1}{2}}) \sim \frac{K_1(\theta^{in})}{2} \hat{u}_1 + O(r^{\frac{1}{2}}), \quad (2.18)$$

and since  $H_1 u^{in} = 0$ ,  $H_1 u^{sc} = \bar{u}_1$  too. Thus, near the tip

$$H_1 u^{sc} - \frac{K_1(\theta^{in})}{2} \hat{u}_1 = O(r^{\frac{1}{2}}) \quad \text{as } r \rightarrow 0 \quad (2.19)$$

and so the left hand side of this equation satisfies the Meixner condition there. It also satisfies the Helmholtz equation, the radiation condition and the Neumann boundary condition on the crack. Thus, uniqueness applies and the left hand side of (2.19) must be identically zero. Hence one arrives at the weak form of embedding,

$$H_1 u^{sc} \equiv \frac{K_1(\theta^{in})}{2} \hat{u}_1, \quad (2.20)$$

and in particular this is true in the far-field, where the asymptotic expansions for  $u^{sc}$  and  $\hat{u}_1$  are given by (2.9) and (2.10), respectively. Hence

$$ik(\cos \theta + \cos \theta^{in})D(\theta, \theta^{in}) = \frac{K_1(\theta^{in})}{2} \hat{D}_1(\theta), \quad (2.21)$$

which, together with equation (2.6) results in the embedding formula

$$D(\theta, \theta^{in}) = -\frac{\hat{D}_1(\theta^{in})\hat{D}_1(\theta)}{\pi k(\cos \theta + \cos \theta^{in})}. \quad (2.22)$$

Of course, this is for a well-known example, but the basic idea and philosophy then carry across to more complicated geometries.

### 2.3 Higher order operator embedding formulae

The embedding formula (2.22) is just one of a family of such formulae. The choice of operator requires some thought and the operators of interest here are those introduced in [II] based on  $T_p$ , the Tchebychev polynomial,

$$H_p = (-ik)^p \left\{ T_p \left( \frac{i}{k} \frac{\partial}{\partial x} \right) - T_p(\cos \theta^{in}) \right\}. \quad (2.23)$$

This  $p$ 'th order differential operator,  $H_p$ , also satisfies the three required properties listed in section 2.2.2. As shown in [II] this operator has an important additional property that will be of use later:

4. It maintains homogeneous (Neumann/Dirichlet) boundary conditions on faces inclined at angles  $q\pi/p$  to the  $x$ -axis, for integer values of  $p$  and  $q$ .

For these higher order operators the calculation is more complicated than for the first order operators, for which the leading order terms of the asymptotic expansions (2.6) sufficed. Applying the operator  $H_p$  to  $u$  near the crack tip now results in

$$\begin{aligned} \bar{u}_p = H_p u &\sim (-ik)^p T_p \left( \frac{i}{k} \frac{\partial}{\partial x} \right) \sum_{j \text{ odd}} K_j(\theta^{in}) S_j + O(r^{\frac{1}{2}}) \\ &\sim \frac{k^p}{2} \sum_{\substack{j=1 \\ j \text{ odd}}}^{2p-1} \frac{K_j(\theta^{in}) B_j \hat{u}_{2p-j}}{B_{j-2p}} + O(r^{\frac{1}{2}}), \end{aligned} \quad (2.24)$$

after making use of the identity

$$T_p \left( \frac{i}{k} \frac{\partial}{\partial x} \right) J_\nu(kr) \cos \nu \theta = \frac{(-i)^p}{2} J_{\nu+p}(kr) \cos(\nu + p)\theta + \frac{i^p}{2} J_{\nu-p}(kr) \cos(\nu - p)\theta, \quad (2.25)$$

noting that  $J_{-j/2}(kr) = -i(-1)^j H_{j/2}(kr) + O(r^{j/2})$  for positive odd integers  $j$ , and explicitly retaining only the overly singular terms. Again noting that  $H_p u^{in} = 0$  so  $H_p u^{sc} = \bar{u}_p$ , and invoking the uniqueness argument, as in the previous subsection, shows that

$$H_p u^{sc} \equiv \frac{k^p}{2} \sum_{\substack{j=1 \\ j \text{ odd}}}^{2p-1} \frac{K_j(\theta^{in}) B_j \hat{u}_{2p-j}}{B_{j-2p}} \quad (2.26)$$

everywhere. The embedding formulae are extracted from this expression by applying the far-field asymptotics using the directivities, and (2.15) as

$$D_p(\theta, \theta^{in}) = \frac{-i^{p+1} \sum_{\substack{j=1 \\ j \text{ odd}}}^{2p-1} \frac{\hat{D}_j(\theta^{in}) B_j \hat{D}_{2p-j}(\theta)}{j B_{j-2p}}}{\pi(T_p(-\cos \theta) - T_p(\cos \theta^{in}))} \quad (2.27)$$

$$\begin{aligned}
& -i \left(\frac{i}{k}\right)^p \sum_{\substack{j=1 \\ j \text{ odd}}}^{2p-1} \hat{D}_j(\theta^{in}) \hat{D}_{2p-j}(\theta) (j-2)(j-4) \dots (j-2(p-1)) \\
& = \frac{\quad}{\pi(T_p(-\cos \theta) - T_p(\cos \theta^{in}))}.
\end{aligned} \tag{2.28}$$

The  $p$  subscript appended to  $D$  denotes that it was determined using the  $p$ 'th order operator. Thus the full directivity is reconstructed from only the knowledge of directivities of the edge Green's functions.

These embedding formulae are more complicated than those obtained using the first order differential operator. In order to check that they do indeed give the same result, numerical values of the directivity  $D_p(\theta, \theta^{in})$  were calculated for  $p = 1, 2, 3$  and  $7$  and various values of  $\theta^{in}$ . The results for different values of  $p$  were indistinguishable and they exhibit the expected singularities at  $\theta = \pi \pm \theta^{in}$ , the angles that form the boundaries of the geometrically reflected partial plane waves and correspond mathematically to a pole coinciding with a stationary phase point when evaluating the far-field, meaning that the cylindrically spreading approximation is invalid there.

That the directivity is the same for *all* orders,  $p$ , of the operator, is proved using induction. Assume first that for some integer value of  $p$  it is true that

$$D_{p-1}(\theta, \theta^{in}) = D_{p-2}(\theta, \theta^{in}) = \dots = D_2(\theta, \theta^{in}) = D_1(\theta, \theta^{in}). \tag{2.29}$$

It can be demonstrated that this is true for  $p = 3$ , using the operator

$$H_2 = \frac{\partial^2}{\partial x^2} + k^2 \cos^2 \theta^{in} \tag{2.30}$$

and working through the details explicitly, so induction can begin. Then the recurrence relation for Tchebychev polynomials **(20)**

$$T_p(x) = 2xT_{p-1}(x) - T_{p-2}(x) \tag{2.31}$$

is applied to the expression for  $\bar{u}_p$  near the crack tip:

$$\begin{aligned}
\bar{u}_p &= (-ik)^p \sum_{j \text{ odd}} K_j(\theta^{in}) \left\{ T_p \left( \frac{i}{k} \frac{\partial}{\partial x} \right) - T_p(\cos \theta^{in}) \right\} S_j \\
&= (-ik)^p \left\{ \frac{2i}{k} \frac{\partial}{\partial x} \sum_{j \text{ odd}} K_j(\theta^{in}) T_{p-1} \left( \frac{i}{k} \frac{\partial}{\partial x} \right) S_j - \sum_{j \text{ odd}} K_j(\theta^{in}) T_{p-2} \left( \frac{i}{k} \frac{\partial}{\partial x} \right) S_j \right\} + O(r^{\frac{1}{2}}) \\
&= 2 \left( \frac{\partial \bar{u}_{p-1}}{\partial x} + (-ik)^{p-1} \sum_{j \text{ odd}} K_j(\theta^{in}) T_{p-1}(\cos \theta^{in}) \frac{\partial S_j}{\partial x} \right) + k^2 \bar{u}_{p-2} + O(r^{\frac{1}{2}}).
\end{aligned} \tag{2.32}$$

The only singular term from  $\partial S_j / \partial x$  occurs when  $j = 1$ , and hence near the tip

$$\bar{u}_p = (-ik)^{p-1} K_1(\theta^{in}) T_{p-1}(\cos \theta^{in}) \hat{u}_1 + 2 \frac{\partial \bar{u}_{p-1}}{\partial x} + k^2 \bar{u}_{p-2} + O(r^{\frac{1}{2}}). \tag{2.33}$$



The uniqueness argument then shows that, everywhere

$$\bar{u}_p \equiv (-ik)^{p-1} K_1(\theta^{in}) T_{p-1}(\cos \theta^{in}) \hat{u}_1 + 2 \frac{\partial \bar{u}_{p-1}}{\partial x} + k^2 \bar{u}_{p-2}. \quad (2.34)$$

This expresses  $\bar{u}_p$  in terms of  $\hat{u}_1$ ,  $\bar{u}_{p-1}$  and  $\bar{u}_{p-2}$ . The directivity of  $\hat{u}_1$  is  $\hat{D}_1(\theta)$ . The directivities of  $\bar{u}_{p-1}$  and  $\bar{u}_{p-2}$  can be written in terms of the directivities for  $u^{sc}$ ,  $D_{p-1}(\theta, \theta^{in})$  and  $D_{p-2}(\theta, \theta^{in})$  respectively, by applying the embedding method with the corresponding operator order. The induction hypothesis, equation (2.29), that the same directivity  $D_1(\theta, \theta^{in})$  is obtained when applying the embedding method for *all* integer orders less than  $p$  thus allows the directivities of  $\bar{u}_{p-1}$  and  $\bar{u}_{p-2}$  to both be written in terms of  $D_1(\theta, \theta^{in})$ . As before,  $H_p u^{in} = 0$ , so  $\bar{u}_p = H_p u^{sc}$  and the directivity for  $u^{sc}$  with the  $p$ 'th order operator is extracted from the far-field behaviour of equation (2.34), since

$$\begin{aligned} & \{T_p(-\cos \theta) - T_p(\cos \theta^{in})\} D_p(\theta, \theta^{in}) \\ &= i \frac{K_1(\theta^{in})}{k} T_{p-1}(\cos \theta^{in}) \hat{D}_1(\theta) - 2 \cos \theta \{T_{p-1}(-\cos \theta) - T_{p-1}(\cos \theta^{in})\} D_{p-1}(\theta, \theta^{in}) \\ & \quad - \{T_{p-2}(-\cos \theta) - T_{p-2}(\cos \theta^{in})\} D_{p-2}(\theta, \theta^{in}) \\ &= i \frac{K_1(\theta^{in})}{k} T_{p-1}(\cos \theta^{in}) \hat{D}_1(\theta) - 2 \cos \theta \{T_{p-1}(-\cos \theta) - T_{p-1}(\cos \theta^{in})\} D_1(\theta, \theta^{in}) \\ & \quad - \{T_{p-2}(-\cos \theta) - T_{p-2}(\cos \theta^{in})\} D_1(\theta, \theta^{in}) \\ &= - [2(\cos \theta + \cos \theta^{in}) T_{p-1}(\cos \theta^{in}) + 2 \cos \theta \{T_{p-1}(-\cos \theta) - T_{p-1}(\cos \theta^{in})\} \\ & \quad + \{T_{p-2}(-\cos \theta) - T_{p-2}(\cos \theta^{in})\}] D_1(\theta, \theta^{in}) \\ &= - [\{2 \cos \theta^{in} T_{p-1}(\cos \theta^{in}) - T_{p-2}(\cos \theta^{in})\} \\ & \quad - \{-2 \cos \theta T_{p-1}(-\cos \theta) - T_{p-2}(-\cos \theta)\}] D_1(\theta, \theta^{in}) \\ &= \{T_p(-\cos \theta) - T_p(\cos \theta^{in})\} D_1(\theta, \theta^{in}), \end{aligned} \quad (2.35)$$

following another application of the recurrence relation (2.31) for Tchebychev polynomials. Thus, as required it has been shown that

$$D_p(\theta, \theta^{in}) = D_1(\theta, \theta^{in}), \quad (2.36)$$

and the final step of the induction process has been achieved showing that this is indeed true for all integer orders of the differential operator. From this one concludes that there is a large family of embedding formulae and the one deduced in [I] is far from unique - although the ultimate directivity, of course, is.

### 3. Embedding formulae for cracks beneath inclined boundaries

We now leave the illustrative Sommerfeld problem for which the directivity is well-known and for which the edge Green's functions are explicit, and address a situation where neither are known in closed form.

The embedding formulae in (2.27) have an additional and highly important property, they involve the differential operator  $H_p$  of (2.23). This operator has additional properties that mean that the embedding formula (2.27) is actually much more general than just holding for a single semi-infinite crack in an infinite body.

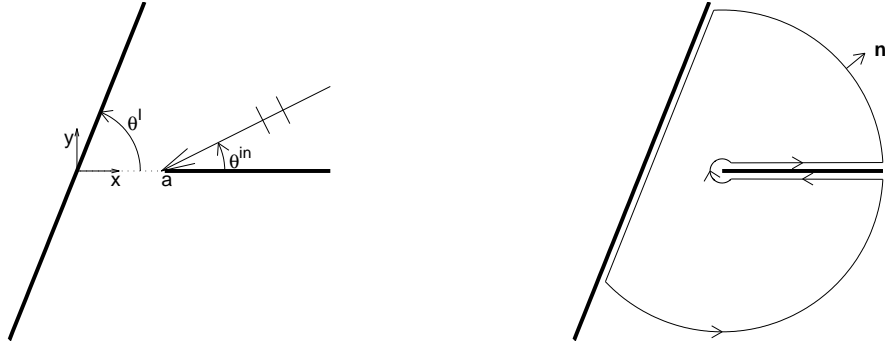


**Fig. 2** The geometry of the inclined boundary and the integration contour for Green's theorem with the semi-infinite crack and inclined boundary.

### 3.1 A semi-infinite crack

We consider the Helmholtz equation (2.1) to now be satisfied in the region to the right of a boundary inclined at angle  $\theta^I$  to the  $x$ -axis, and the crack occupies  $y = 0$ ,  $x > a$ , as shown in figure 2. The Neumann boundary condition  $\partial u / \partial n = 0$  holds on both planar surfaces, and the system is excited by a plane wave incident at angle  $\theta^{in}$ . It is convenient to include the plane wave reflected at the inclined boundary as part of the disturbance incident on the crack:

$$u^{in} = \exp[-ik(x \cos \theta^{in} + y \sin \theta^{in})] + \exp[ik(x \cos(\theta^{in} - 2\theta^I + \pi) - y \sin(\theta^{in} - 2\theta^I + \pi))]. \quad (3.1)$$

If the inclination of the boundary is restricted to be a 'rational' angle,

$$\theta^I = q\pi/p \quad (3.2)$$

for integer values of  $q$  and  $p$ , then the analysis of section 2 can be extended to this case. We define the edge Green's function,  $\hat{u}_j$ , to be a solution of the Helmholtz equation that satisfies the boundary conditions (Neumann on the semi-infinite crack and inclined surface) exactly. The edge Green's function has the edge asymptotics that  $\hat{u}_j \sim r^{-j/2}$  as  $r \rightarrow 0$  and it is convenient to keep the same form of solution as in the previous section

$$\hat{u}_j = A_j H_{j/2}(kr) \cos\left(\frac{j\theta}{2}\right) + O(r^{1/2}), \quad A_j = \frac{i\pi}{\Gamma(j/2)} \left(\frac{k}{2}\right)^{j/2}, \quad j = 1, 3, 5, \dots \quad (3.3)$$

near the origin. Notably, however, although the local behaviour near the origin has the same form as in the previous section we have no recourse to the exact solution when the inclined boundary is present. In the far field

$$\hat{u}_j \sim \hat{D}_j(\theta) \frac{\exp[i(kr - \frac{\pi}{4})]}{(2\pi kr)^{1/2}}.$$

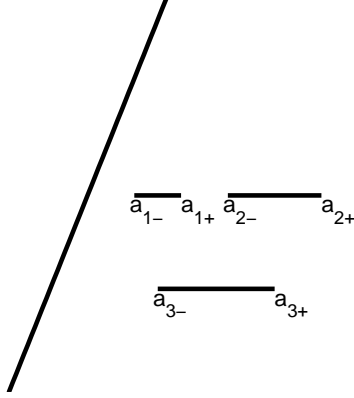


**Fig. 3** Geometry of the inclined boundary and finite parallel cracks.

The main difference with the Sommerfeld example is that the directivity  $\hat{D}_j$  is no longer given exactly as in equation (2.11), but now must be obtained as the solution of an integral equation, i.e. numerically.

To derive the embedding formulae Green's theorem is applied to the modified contour shown in figure 2, and again this results in equation (2.15), where  $\mathcal{L}$  now comprises all the straight parts of the contour. However, since  $\partial u^{in}/\partial n = 0$  on the inclined boundary, by construction, and it is also *required* that  $\partial \hat{u}_j/\partial n = 0$  there too,  $\mathcal{L}$  may be regarded as comprising only the straight portions of the contour parallel to the semi-infinite crack, and thus is the same contour as when the inclined boundary is absent.

The embedding formula for this problem is then obtained using the differential operator  $H_p$  defined by equation (2.23) with  $p$  given by equation (3.2). This operator has the required properties that  $H_p u^{in} = 0$  for this problem and  $H_p u$  is a solution of the Helmholtz equation which satisfies the Neumann boundary condition on both the crack surface and the inclined boundary. Then, the analysis detailed in equations (2.24,2.26) applies in this case, and hence the embedding formula is again given by equation (2.27), with suitable functions  $\hat{D}_j$  and the directivity for any combination of incident or observation angles can be calculated as a combination of the  $p$  functions  $\hat{D}_j(\theta)$ ,  $j = 1, 3, \dots, (2p - 1)$ .

### 3.2 Finite and multiple planar cracks

The previous result is now generalised to the case of  $N$  parallel finite length cracks,  $a_{l-} < x < a_{l+}$ ,  $y = y_l$ ,  $l = 1, 2, \dots, N$ , together with the inclined boundary, as shown in figure 3, on all of which the Neumann boundary conditions are satisfied. The embedding method described above is generalised by defining  $p$  edge Green's functions at each end of each of the  $N$  cracks. Thus, for the functions associated with the  $l$ 'th crack,

$$\hat{u}_j(\mathbf{x}; a_{l\pm}) = A_j H_{j/2}(k\rho_{a_{l\pm}}) \cos\left(\frac{j\theta_{a_{l\pm}}}{2}\right) + O(\rho_{a_{l\pm}}^{\frac{1}{2}}), \quad \text{as } \rho_{a_{l\pm}} \rightarrow 0$$

$$j = 1, 3, \dots, (2p - 1), \quad l = 1, 2, 3, \dots, N \quad (3.4)$$

where  $\rho_{a_{l\pm}}, \theta_{a_{l\pm}}$  are local polar coordinates relative to the ends  $a_{l\pm}$  of the  $l$ 'th crack (with the angular axis locally orientated so that  $0 < \theta_{a_{l\pm}} < 2\pi$  measured in the anticlockwise sense). Also the functions  $\hat{u}_j(\mathbf{x}; a_{l\pm})$  are required to satisfy the Neumann boundary condition on the inclined boundary and on *all* the finite cracks. The directivity of these edge Green's functions are denoted by  $\hat{D}_j(\theta; a_{l\pm})$ .

Similarly, the asymptotic behaviour of the total field near the crack edge (2.4) is generalised to

$$u \sim \sum_{j \text{ odd}} K_j(\theta^{in}; a_{l\pm}) B_j J_{j/2}(k\rho_{a_{l\pm}}) \cos\left(\frac{j\theta_{a_{l\pm}}}{2}\right), \quad \text{as } \rho_{a_{l\pm}} \rightarrow 0, \quad l = 1, 2, 3, \dots, N. \quad (3.5)$$

Green's theorem is then applied to  $u^{sc}$  with each of the edge Green's functions in turn. Then

$$\pi j K_j(\theta^{in}; a_{l\pm}) = \int_{\mathcal{L}} \left( \hat{u}_j(\mathbf{x}; a_{l\pm}) \frac{\partial}{\partial n} u^{sc} - u^{sc} \frac{\partial}{\partial n} \hat{u}_j(\mathbf{x}; a_{l\pm}) \right) ds = -2i \hat{D}_j(\theta^{in}; a_{l\pm}). \quad (3.6)$$

where  $\mathcal{L}$  is now the total of *all* the planar crack surfaces.

As in the previous section the differential operator  $H_p$  is then applied to the physical solution  $u$ , and generates an edge Green's function, with  $p$  different orders of singularity at each end of each of the cracks. Near any particular left hand end crack tip  $x = a_{l-}$ ,  $\bar{u}_p$  has asymptotic behaviour given by (2.24) with the appropriate generalisation of the notation. Near any particular right hand end crack tip  $x = a_{l+}$ , each differentiation with respect to  $x$  introduces a sign change and hence near to  $a_{l+}$  the asymptotic behaviour of  $\bar{u}_p$  is

$$\bar{u}_p \sim \frac{(-k)^p}{2} \sum_{\substack{j=1 \\ j \text{ odd}}}^{2p-1} \frac{K_j(\theta^{in}; a_{l+}) B_j \hat{u}_{2p-j}(\mathbf{x}; a_{l+})}{B_{j-2p}} + O(\rho_{a_{l+}}^{\frac{1}{2}}). \quad (3.7)$$

Hence, invoking uniqueness again

$$\bar{u}_p \equiv \frac{k^p}{2} \sum_{\substack{j=1 \\ j \text{ odd}}}^{2p-1} \frac{B_j [K_j(\theta^{in}; a_{l-}) \hat{u}_{2p-j}(\theta; a_{l-}) + (-1)^p K_j(\theta^{in}; a_{l+}) \hat{u}_{2p-j}(\theta; a_{l+})]}{B_{j-2p}} \quad (3.8)$$

from which the directivity is extracted as

$$D_p(\theta, \theta^{in}) = \frac{-i}{(T_p(-\cos\theta) - T_p(\cos\theta^{in}))} \left(\frac{i}{k}\right)^p \sum_{l=1}^N \sum_{\substack{j=1 \\ j \text{ odd}}}^{2p-1} \left[ \hat{D}_j(\theta^{in}; a_{l-}) \hat{D}_{M-j}(\theta; a_{l-}) + (-1)^p \hat{D}_j(\theta^{in}; a_{l+}) \hat{D}_{M-j}(\theta; a_{l+}) \right] (j-2)(j-4) \dots (j-M+2), \quad (3.9)$$

with  $M = 2p$ . In the particular case that  $\theta^I = 0$ , this problem reduces to that of parallel finite cracks below a parallel boundary and the formula above reduces to that given in [I].

#### 4. Linear superposition

An interesting re-modelling of the embedding formulae of papers I & II is given in (17) in which it is noted that overly singular eigenfunctions (edge Green's functions) are not very convenient in many numerical schemes, although they are analytically and physically more appealing. Non-singular standard solutions, for an incoming plane wave (or finite number of waves) are used in (17), together with the operators  $H_p$  to recast the embedding formulae of paper II into this numerically more convenient form. As this approach uses multiple plane wave scattering problems the notation now includes additional subscripts to denote the incident angle of the plane wave. For illustration we first revisit the Sommerfeld problem of section 2 and apply both first order and higher order operators to generate embedding formulae, and then show how these are related to those for more general cracks (semi-infinite plus boundary and multiple finite cracks).

##### 4.1 First order operator embedding formula

In order to obtain the embedding formula using superposition of plane wave solutions the notation is changed slightly. The differential operator [I] associated with incident angle  $\theta^{in}$  is denoted here as

$$H_{1,\theta^{in}} = \frac{\partial}{\partial x} + ik \cos \theta^{in}, \quad (4.1)$$

and the scattered field associated with this incident angle is denoted here  $u_{in}^{sc}(r, \theta, \theta^{in})$ . Near to the crack tip, the asymptotic behaviour of the total field is

$$u_{in}(r, \theta, \theta^{in}) \sim K_1(\theta^{in}) r^{\frac{1}{2}} \cos\left(\frac{\theta}{2}\right) + O(r^{\frac{3}{2}}). \quad (4.2)$$

As with the edge Green's function method

$$H_{1,\theta^{in}} u_{in}(r, \theta, \theta^{in}) \sim \frac{K_1(\theta^{in})}{2r^{\frac{1}{2}}} \cos\left(\frac{\theta}{2}\right) + O(r^{\frac{1}{2}}), \quad (4.3)$$

and since  $H_{1,\theta^{in}} u_{in}^{in} = 0$ , near the tip it is also true that

$$H_{1,\theta^{in}} u_{in}^{sc} \sim \frac{K_1(\theta^{in})}{2r^{\frac{1}{2}}} \cos\left(\frac{\theta}{2}\right) + O(r^{\frac{1}{2}}), \quad (4.4)$$

which exhibits a singularity there. Similarly, for a wave incident at a different angle,  $\theta_1$ , say

$$H_{1,\theta_1} u_1^{sc} \sim \frac{K_1(\theta_1)}{2r^{\frac{1}{2}}} \cos\left(\frac{\theta}{2}\right) + O(r^{\frac{1}{2}}), \quad (4.5)$$

which also exhibits a singularity of the same order as  $r \rightarrow 0$ . Hence these expressions are combined in such a way as to eliminate the singularity there:

$$H_{1,\theta_1} u_1^{sc} - \frac{K_1(\theta_1)}{K_1(\theta^{in})} H_{1,\theta^{in}} u_{in}^{sc} = O(r^{\frac{1}{2}}). \quad (4.6)$$

From the properties of the operators  $H_{1,\theta_j}$  it is clear that the left hand side of this equation is a solution of the Helmholtz equation which satisfies the radiation condition and the Meixner condition at the tip. As each term on the left hand side individually satisfies the Neumann boundary condition on the crack it is clear that their combination also satisfies the boundary condition there. Thus, uniqueness applies and the left hand side must be identically zero, hence everywhere

$$H_{1,\theta_1} u_1^{sc} \equiv \frac{K_1(\theta_1)}{K_1(\theta^{in})} H_{1,\theta^{in}} u_{in}^{sc}. \quad (4.7)$$

In particular this must be true in the far-field, where the asymptotic expansions for  $u_{in}^{sc}$  and  $u_1^{sc}$  apply; thus

$$ik(\cos \theta + \cos \theta_1) D(\theta, \theta_1) = \frac{K_1(\theta_1)}{K_1(\theta^{in})} ik(\cos \theta + \cos \theta^{in}) D(\theta, \theta^{in}). \quad (4.8)$$

This must be true for *all* values of  $\theta$ , and setting  $\theta = \theta_1$ , we obtain

$$2 \cos \theta_1 D(\theta_1, \theta_1) = \frac{K_1(\theta_1)}{K_1(\theta^{in})} (\cos \theta_1 + \cos \theta^{in}) D(\theta_1, \theta^{in}). \quad (4.9)$$

The principle of reciprocity ensures that  $D(\theta_1, \theta^{in}) = D(\theta^{in}, \theta_1)$  and hence  $K_1(\theta_1)/K_1(\theta^{in})$  can be expressed in terms of the directivity of the scattered field with incident angle  $\theta_1$  as

$$\frac{K_1(\theta_1)}{K_1(\theta^{in})} = \frac{2 \cos \theta_1 D(\theta_1, \theta_1)}{(\cos \theta_1 + \cos \theta^{in}) D(\theta^{in}, \theta_1)}. \quad (4.10)$$

Substituting this into equation (4.8) allows the directivity for any incident angle  $\theta^{in}$  for which  $\cos \theta^{in} + \cos \theta_1 \neq 0$  to be expressed in terms of the directivity for incident angle  $\theta_1$  via the embedding formula

$$D(\theta, \theta^{in}) = \frac{(\cos \theta + \cos \theta_1)(\cos \theta_1 + \cos \theta^{in})}{2 \cos \theta_1 (\cos \theta + \cos \theta^{in})} \frac{D(\theta, \theta_1) D(\theta^{in}, \theta_1)}{D(\theta_1, \theta_1)}. \quad (4.11)$$

In the special case for which  $\cos \theta^{in} + \cos \theta_1 = 0$  the factor  $(\cos \theta_1 + \cos \theta^{in}) D(\theta^{in}, \theta_1)$  should be replaced in equation (4.11) by the (finite) limiting value of  $(\cos \theta_1 + \cos \hat{\theta}) D(\hat{\theta}, \theta_1)$  as  $\cos \hat{\theta} \rightarrow -\cos \theta_1$ . Equation (4.11) appears to be a different embedding formula to that obtained using edge Green's functions, equation (2.22), which structurally it certainly is, but the resulting directivity is the same as that found earlier. It is analytically a bit more cumbersome and arguably a little less elegant, but overly singular states have never been introduced. This formula simply states that given the directivity for the standard problem of an incoming plane wave for a single incident angle  $\theta_1$ , those for all other incident angles can be deduced.

#### 4.2 Higher order operator embedding formulae

The higher order differential operators based on the Tchebychev polynomial,

$$H_{p,\theta^{in}} = (-ik)^p \left\{ T_p \left( \frac{i}{k} \frac{\partial}{\partial x} \right) - T_p(\cos \theta^{in}) \right\}, \quad (4.12)$$

can also be used with linear superposition as indeed is done in (17) for the wedge-like geometries of paper II. As noted previously, this operator maintains homogeneous boundary conditions, not only on the  $x$ -axis, but also on faces inclined at angles  $q\pi/p$  to the  $x$ -axis for integer values of  $p$  and  $q$ . As with the edge Green's function method, near the crack tip

$$\begin{aligned} H_{p,\theta^{in}}u_{in}(r,\theta,\theta^{in}) &\sim (-ik)^p T_p \left( \frac{i}{k} \frac{\partial}{\partial x} \right) \sum_{j \text{ odd}} K_j(\theta^{in}) S_j + O(r^{\frac{1}{2}}) \\ &\sim \frac{k^p}{2} \sum_{\substack{j=1 \\ j \text{ odd}}}^{2p-1} K_j(\theta^{in}) B_j f_{\frac{j-2p}{2}}(r,\theta) + O(r^{\frac{1}{2}}), \end{aligned} \quad (4.13)$$

in which only the overly singular terms have been explicitly retained, and where,  $f_{\frac{j}{2}} = J_{\frac{j}{2}}(kr) \cos(j\theta/2)$ . Again noting that  $H_{p,\theta^{in}}u_{in}^{in} = 0$  we deduce that

$$H_{p,\theta^{in}}u_{in}^{sc} \sim \frac{k^p}{2} \sum_{\substack{j=1 \\ j \text{ odd}}}^{2p-1} K_j(\theta^{in}) B_j f_{\frac{j-2p}{2}}(r,\theta) + O(r^{\frac{1}{2}}). \quad (4.14)$$

Each of the terms in this summation has singularities of orders  $O(r^{-\frac{1}{2}})$ ,  $O(r^{-\frac{3}{2}})$ ,  $\dots$ ,  $O(r^{-\frac{(2p-j)}{2}})$ , and consequently  $H_{p,\theta^{in}}u_{in}^{sc}$  also has singularities of orders  $O(r^{-\frac{1}{2}})$ ,  $O(r^{-\frac{3}{2}})$ ,  $\dots$ ,  $O(r^{-\frac{(2p-1)}{2}})$ . Similar expressions are also derived for the operators  $H_{p,\theta_l}$  defined for angles  $\theta_l$ ,  $l = 1, 2, \dots, p$ :

$$H_{p,\theta_l}u_l^{sc} \sim \frac{k^p}{2} \sum_{\substack{j=1 \\ j \text{ odd}}}^{2p-1} K_j(\theta_l) B_j f_{\frac{j-2p}{2}}(r,\theta) + O(r^{\frac{1}{2}}). \quad (4.15)$$

These expressions are now combined in such a way as to eliminate all  $p$  orders of singularity, or equivalently to eliminate the  $p$  functions  $f_{\frac{j}{2}-l}$ ; thus

$$H_{p,\theta^{in}}u_{in}^{sc} - \sum_{l=1}^p X_l H_{p,\theta_l}u_l^{sc} \sim O(r^{\frac{1}{2}}), \quad (4.16)$$

for some values  $X_l$ ,  $l = 1, 2, \dots, p$ , still to be determined. From the properties of the operators  $H_{p,\theta_j}$  it is clear that the left hand side of equation (4.16) is a solution of the Helmholtz equation which satisfies the radiation condition and the Meixner condition at the tip. As each term on the left hand side individually satisfies the Neumann boundary condition on the crack it is clear that their combination also satisfies the boundary condition there. Thus, uniqueness applies and the left hand side must be identically zero, hence everywhere

$$H_{p,\theta^{in}}u_{in}^{sc} \equiv \sum_{l=1}^p X_l H_{p,\theta_l}u_l^{sc}. \quad (4.17)$$

In particular this must be true in the far-field, where the asymptotic expansions for  $u_{in}^{sc}$  and  $u_l^{sc}$ ,  $l = 1, 2, \dots, p$ , apply, resulting in

$$(T_p(-\cos\theta) - T_p(\cos\theta^{in}))D_p(\theta, \theta^{in}) = \sum_{l=1}^p X_l(T_p(-\cos\theta) - T_p(\cos\theta_l))D_p(\theta, \theta_l). \quad (4.18)$$

The values of  $X_l$  are found by setting  $\theta = \theta_l$ ,  $l = 1, 2, \dots, p$  in turn, as the solution of the matrix equation

$$\begin{array}{ccc} M & X & = & F \\ (p \times p) & (p \times 1) & & (p \times 1) \end{array} \quad (4.19)$$

where

$$M_{jl} = (T_p(-\cos\theta_j) - T_p(\cos\theta_l))D_p(\theta_j, \theta_l), \quad (4.20)$$

$$F_j = (T_p(-\cos\theta_j) - T_p(\cos\theta^{in}))D_p(\theta^{in}, \theta_j). \quad (4.21)$$

Thus, the embedding formulae are written in matrix form as

$$D_p(\theta, \theta^{in}) = \left\{ \begin{array}{cc} N & M^{-1} \\ (1 \times p) & (p \times p) \end{array} \right\} \begin{array}{c} F \\ (p \times 1) \end{array} / (T_p(-\cos\theta) - T_p(\cos\theta^{in})), \quad (4.22)$$

where

$$N_{1l} = (T_p(-\cos\theta) - T_p(\cos\theta_l))D_p(\theta, \theta_l). \quad (4.23)$$

It can be shown using an induction argument that, as for the edge Green's function method, this ultimately gives the same directivity for *all* orders of the operator.

Exactly as in section 4 one directly extends this to a semi-infinite crack beneath an inclined boundary by noting that the operator  $H_p$  maintains homogeneous boundary conditions, not only on the  $x$ -axis, but also on the face inclined at angle  $q\pi/p$  to the  $x$ -axis, as required here. From the construction of  $u_{in}^{in}$ ,

$$u_{in}^{in} = \exp[-ik(x \cos\theta^{in} + y \sin\theta^{in})] + \exp[ik(x \cos(\theta^{in} - 2\theta^I + \pi) - y \sin(\theta^{in} - 2\theta^I + \pi))], \quad (4.24)$$

the important property

$$H_{p,\theta^{in}} u_{in}^{in} = 0 \quad (4.25)$$

is also maintained. The embedding formula (4.22) then follows using the far-field directivities and setting  $\theta$  in turn to  $\theta_l$ ,  $l = 1, 2, \dots, p$ , to eliminate the coefficients  $X_l$ . Of course, in using (4.22) for the subsurface inclined crack one must now use reference directivities found in the presence of the boundary.

### 4.3 Finite subsurface crack(s)

We now move on to consider  $N$  parallel finite length cracks,  $a_{l-} < x < a_{l+}$ ,  $y = y_l$ ,  $l = 1, 2, \dots, N$ , together with the inclined boundary, as shown in figure 3, on all of which the Neumann boundary conditions are satisfied. Due to the slope of the inclined boundary the  $p$ 'th order differential operators are again applied. However,  $2Np$  reference plane-wave scattering solutions are needed – these arise because there are  $p$  orders of singularity at each end of each of the  $N$  cracks, which need to be eliminated. Each of these plane wave scattering



solutions must satisfy the Neumann boundary conditions on *all* of the planar surfaces. The plane wave which is reflected at the inclined boundary is again included as part of the incident disturbance, so  $u_{in}^{in}$  is (4.24), and near the crack tips the asymptotic behaviour of the total field,  $u_{in}$  is given by (3.5) and the notation  $\rho_{a_{l\pm}}$ ,  $\theta_{a_{l\pm}}$  etc are as in section 3.2. Applying the differential operator near the crack tip, and noting that  $H_{p,\theta^{in}}u_{in}^{in} = 0$ , we find that

$$H_{p,\theta^{in}}u_{in}^{sc}(\mathbf{x}; a_{l\pm}) \sim \frac{(\mp k)^p}{2} \sum_{\substack{j=1 \\ j \text{ odd}}}^{2p-1} K_j(\theta^{in}; a_{l\pm}) B_j f_{\frac{i-2p}{2}}(\rho_{a_{l\pm}}, \theta_{a_{l\pm}}) + O(\rho_{a_{l\pm}}^{\frac{1}{2}}). \quad (4.26)$$

Each of the terms in this summation has singularities of orders  $O(\rho_{a_{l\pm}}^{-\frac{1}{2}})$ ,  $O(\rho_{a_{l\pm}}^{-\frac{3}{2}})$ ,  $\dots$ ,  $O(\rho_{a_{l\pm}}^{-\frac{(2p-j)}{2}})$ , and consequently  $H_{p,\theta^{in}}u_{in}^{sc}(\mathbf{x}; a_{l\pm})$  also has singularities of orders  $O(\rho_{a_{l\pm}}^{-\frac{1}{2}})$ ,  $O(\rho_{a_{l\pm}}^{-\frac{3}{2}})$ ,  $\dots$ ,  $O(\rho_{a_{l\pm}}^{-\frac{(2p-1)}{2}})$ . Similar expressions are also derived for the operators  $H_{p,\theta_L}$  defined for angles  $\theta_L$ ,  $L = 1, 2, \dots, 2Np$ :

$$H_{p,\theta_L}u_L^{sc}(\mathbf{x}; a_{l\pm}) \sim \frac{(\mp k)^p}{2} \sum_{\substack{j=1 \\ j \text{ odd}}}^{2p-1} K_j(\theta_L; a_{l\pm}) B_j f_{\frac{i-2p}{2}}(\rho_{a_{l\pm}}, \theta_{a_{l\pm}}) + O(\rho_{a_{l\pm}}^{\frac{1}{2}}). \quad (4.27)$$

These expressions are combined in such a way as to eliminate all  $p$  orders of singularity at each of the  $2N$  crack tip locations, or equivalently to eliminate the  $2Np$  functions  $f_{\frac{1}{2}-L}(\rho_{a_{l\pm}}, \theta_{a_{l\pm}})$ . Thus, it is required that

$$H_{p,\theta^{in}}u_{in}^{sc}(\mathbf{x}; a_{l\pm}) - \sum_{L=1}^{2Np} X_L H_{p,\theta_L}u_L^{sc}(\mathbf{x}; a_{l\pm}) \sim O(\rho_{a_{l\pm}}^{\frac{1}{2}}) \quad \text{as } \rho_{a_{l\pm}} \rightarrow 0, \quad l = 1, 2, \dots, N, \quad (4.28)$$

for some values  $X_L$ ,  $L = 1, 2, \dots, 2Np$ , still to be determined. From the properties of the operators  $H_{p,\theta_j}$  it is clear that the left hand side of equation (4.28) is a solution of the Helmholtz equation which satisfies the radiation condition and the Meixner condition at each of the crack tips. As each term on the left hand side individually satisfies the Neumann boundary condition on the crack it is clear that their combination also satisfies the boundary condition there. Thus, uniqueness applies and the left hand side must be identically zero, hence everywhere

$$H_{p,\theta^{in}}u_{in}^{sc} \equiv \sum_{L=1}^p X_L H_{p,\theta_L}u_L^{sc}. \quad (4.29)$$

In particular this must be true in the far-field, where the asymptotic expansions for  $u_{in}^{sc}$  and  $u_L^{sc}$ ,  $L = 1, 2, \dots, 2Np$ , apply and it is found that

$$(T_p(-\cos\theta) - T_p(\cos\theta^{in}))D(\theta, \theta^{in}) = \sum_{L=1}^{2Np} X_L (T_p(-\cos\theta) - T_p(\cos\theta_L))D(\theta, \theta_L). \quad (4.30)$$

The values of  $X_L$  are found by setting  $\theta = \theta_L$ ,  $L = 1, 2, \dots, 2Np$  in turn, as the solution of the matrix equation

$$\begin{array}{ccc} M & X & = & F \\ (2Np \times 2Np) & (2Np \times 1) & & (2Np \times 1) \end{array} \quad (4.31)$$

where

$$M_{jL} = (T_p(-\cos\theta_j) - T_p(\cos\theta_L))D(\theta_j, \theta_L), \quad (4.32)$$

$$F_j = (T_p(-\cos\theta_j) - T_p(\cos\theta^{in}))D(\theta^{in}, \theta_j). \quad (4.33)$$

Thus, the embedding formula is written in matrix form as

$$D(\theta, \theta^{in}) = \left\{ \begin{array}{cc} N & M^{-1} \\ (1 \times 2Np) & (2Np \times 2Np) \end{array} \right\} F \quad / (T_p(-\cos\theta) - T_p(\cos\theta^{in})), \quad (4.34)$$

where

$$N_{1L} = (T_p(-\cos\theta) - T_p(\cos\theta_L))D(\theta, \theta_L). \quad (4.35)$$

## 5. Numerical implementations

As noted earlier embedding formulae would simply be a mathematical curiosity if they were not implementable. To illustrate their practicality we briefly describe their numerical implementation here.

### 5.1 Edge Green's function

In [1] we used integral equations to formulate and solve for scattering by a single finite crack in an infinite domain using a Tchebychev expansion and the properties of generalised functions; this was for the  $p = 1$  operator. The extension to higher  $p$  has eluded us, due to the generalised functions, and so we implement another approach: collocation. The explicit computation of the edge Green's function in the framework of the collocation scheme requires us to overcome certain technical difficulties. Namely, the presence of functions that are oversingular, i.e. with non-integrable singularities, leads to divergent integrals. Here we demonstrate how to evaluate integral equations containing edge Green's functions.

For clarity we consider the simplest case, namely the Dirichlet problem, and consider the scatterers to be composed from several segments. The Dirichlet problem is chosen since this integral equation itself has an integrable kernel, so it does not require any regularization. The Neumann problem contains some additional difficulties. We denote the scatterers by  $\mathcal{L}$ . It is well known that for such a problem, with plane wave incidence, the integral equation

$$\int_{\mathcal{L}} \psi(\mathbf{r}') G(|\mathbf{r} - \mathbf{r}'|) d\mathbf{r}' = -u^{in}(\mathbf{r}), \quad \mathbf{r} \in \mathcal{L}, \quad (5.1)$$

emerges, where  $G(r) = -\frac{i}{4}H_0^{(1)}(kr)$  is the free space Green's function, and  $\psi(\mathbf{r})$  is the unknown potential density (it is equal to the difference of the normal derivatives of the field taken on different faces of the scatterer). The directivity of the scattered field can be calculated via the formula

$$D(\theta, \theta^{in}) = -i \int_{\mathcal{L}} \psi(\mathbf{r}) p(\theta, \mathbf{r}) d\mathbf{r}, \quad (5.2)$$

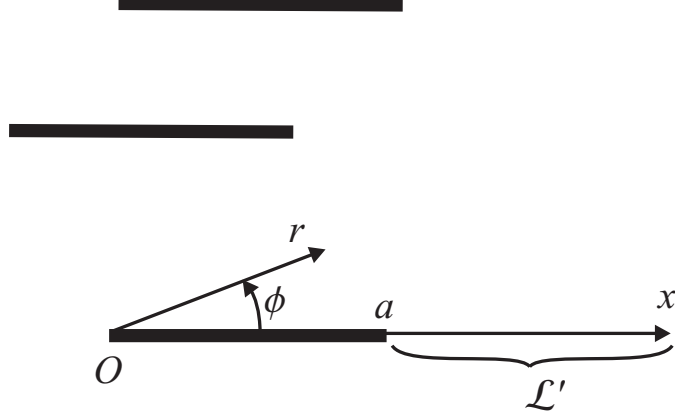


**Fig. 4** The geometrical notation for the numerical calculation of the edge Green's function

where  $p(\theta, \mathbf{r}) = \exp\{-ik(x \cos \theta + y \sin \theta)\}$ , and  $(x, y)$  are the coordinates of  $\mathbf{r}$ . If we now have an edge Green's function, with index  $j$ , then again an integral equation can be formally written down. For simplicity we let the edge, at which the singularity of the edge Green's function is located, coincide with the origin of the coordinate system, and the segment of the scatterer on which it is located lie on the positive  $x$ -axis (see Fig 4). We represent the unknown function  $\hat{\psi}(\mathbf{r})$  in the form  $\hat{\psi} = \hat{\psi}_r + \hat{\psi}_s$ , where  $\hat{\psi}_r$  is the "regular" part of the function growing no faster than  $r^{-1/2}$  at the vicinities of the edges,  $r$  being the local radial coordinate to the edge, and  $\hat{\psi}_s$  is the "singular" part. The singular piece is set equal to zero on all segments except the one to which the origin belongs and on this last segment it coincides with the jump of the normal derivative of the half-line edge Green's function; thus

$$\hat{\psi}_s(x) = \Psi(x) = \frac{jA_j}{2x} H_{j/2}^{(1)}(kx) \quad \text{for } 0 < x < a. \quad (5.3)$$

The integral equation for the edge Green's function can be written in the following form:

$$\int_{\mathcal{L}} G(|\mathbf{r} - \mathbf{r}'|) \hat{\psi}_r(\mathbf{r}') d\mathbf{r}' = - \int_{\mathcal{L}} G(|\mathbf{r} - \mathbf{r}'|) \hat{\psi}_s(\mathbf{r}') d\mathbf{r}', \quad (5.4)$$

where the integrals containing  $\hat{\psi}_s$  are regularized by subtracting out the known form (5.3). Noting that

$$\int_0^\infty \Psi(\mathbf{r}') G(|\mathbf{r} - \mathbf{r}'|) d\mathbf{r}' = U(\mathbf{r}) \equiv A_j H_{j/2}^{(1)}(kr) \sin(j\phi/2) \quad (5.5)$$

where the integration is held over the positive  $x$  axis then the function  $U$  is none other than the half-line edge Green's function. Everywhere on  $\mathcal{L}$  the function  $U(\mathbf{r})$  is regular, since on the positive  $x$  half-axis it is equal to zero. Now equation (5.4) can be rewritten as follows

$$\int_{\mathcal{L}} G(|\mathbf{r} - \mathbf{r}'|) \hat{\psi}_r(\mathbf{r}') d\mathbf{r}' = \int_{\mathcal{L}'} G(|\mathbf{r} - \mathbf{r}'|) \Psi(\mathbf{r}') d\mathbf{r}' - U(\mathbf{r}). \quad (5.6)$$

where  $\mathcal{L}'$  is the line  $y = 0$ ,  $a < x < \infty$ . The integrals in (5.6) are now convergent and this equation is solved numerically to find  $\hat{\psi}_r$ .

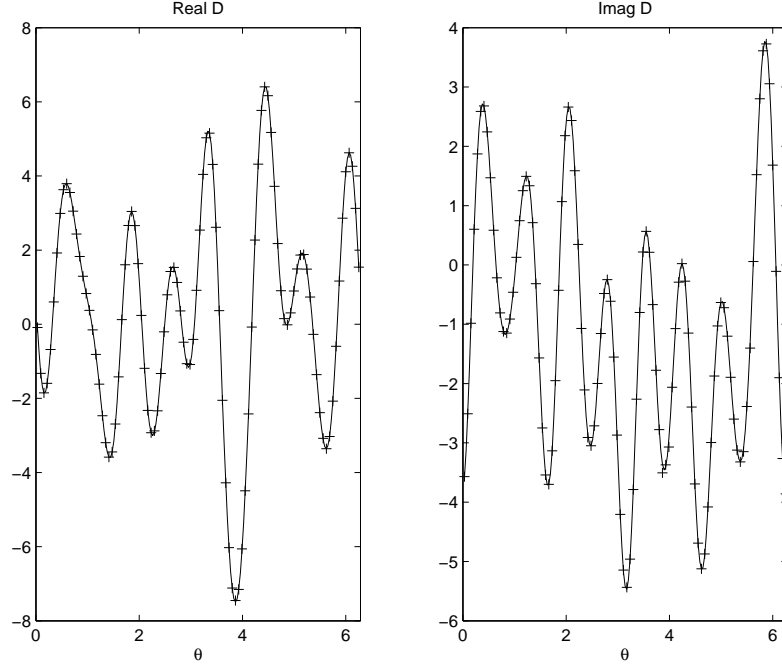


**Fig. 5** A numerical implementation of the collocation scheme: solid lines are from a direct calculation and the crosses are the directivity found using edge Green's functions.

After finding  $\hat{\psi}_r$  the directivity  $\hat{D}$  associated with the edge Green's function is evaluated by quadrature as

$$\hat{D}(\theta) = -i \int_{\mathcal{L}} \hat{\psi}_r(\mathbf{r}) p(\theta, \mathbf{r}) d\mathbf{r} + i \int_{\mathcal{L}'} \Psi(\mathbf{r}) p(\theta, \mathbf{r}) d\mathbf{r} + 2A_j e^{-ij\pi/2} \sin(j\theta/2). \quad (5.7)$$

The results from a numerical implementation of this scheme are shown in figure 5; the specific example is that of two Dirichlet strips each of length  $2a$ , one on  $x = 0$ ,  $a < y < 3a$  and the other  $y = 0$ ,  $a < x < 3a$ . The problem can thus be solved using the  $p = 2$  operator. The other parameters used in the figure,  $ka = \pi$  and  $\theta^{in} = \pi/4.12$ , are simply representative of typical values.

## 5.2 Linear superposition

The advantage of linear superposition is that any existing numerical scheme can be utilised and one just needs a finite number of directivities from it for specific  $\theta^{in}$  to reconstruct the whole directivity for all  $\theta, \theta^{in}$ . We use the Galerkin, scheme described in detail in (21) which solves for plane wave incidence upon a Neumann crack beneath an inclined Neumann interface. The full directivity (for all  $\theta, \theta^{in}$ ) is shown in figure 6 for a crack of inclination  $\pi/4$  and thus the  $p = 4$  operator is required. One takes 8 directivity patterns, these are each for a fixed  $\theta^{in}$  and all  $\theta$ , (i.e. all one requires are 8 vertical slices through figure 6 to construct the whole figure) then formulae (4.34,4.35) are used; these are easy to implement, and thus

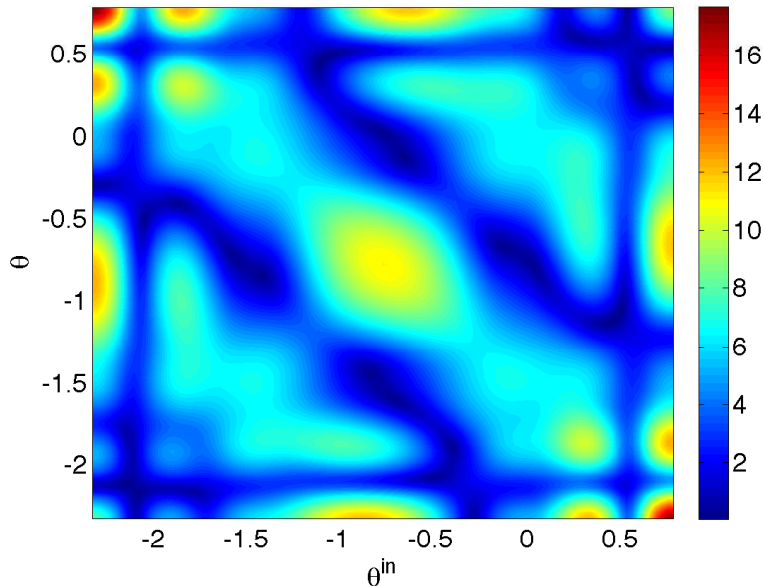


**Fig. 6** The directivity,  $|D(\theta, \theta^{in})|$ , for a finite crack of length  $2a$ ,  $ka = 3$ , whose center is a perpendicular distance  $d = 2a$  from a plane inclined with  $\theta_l = \pi/4$ .

the full directivity emerges almost immediately. The computational cost is minimal, in contrast calculating the same figure directly is more intensive as each directivity for the hundred values of  $\theta^{in}$  used to create that figure must then be individually calculated.

## 6. Coupled differential operators

### 6.1 Two perpendicular strips

To further demonstrate the utility of our formulae we consider scattering by two strips located at right angles to each other (see figure 7). We could use the  $p = 2$  operator as in the main text and in the numerical example of section 5.1, but we will use this example to illustrate a slightly different idea in which we introduce two physical problems that share the same geometry, but that now differ in the boundary conditions on one strip. They then each have their edge Green's function counterparts. The embedding formula is then generated by applying two differential operators of first order.

The Dirichlet boundary condition  $u = 0$  is assumed to hold on the faces of the segments (strips) 1–2 and 3–4, Meixner's conditions are valid at the edges, and the radiation condition for the scattered field holds at infinity. The total field is decomposed into an incident plane wave and the scattered field where the incident field has the form (2.2), and the scattered field as  $r \rightarrow \infty$  is

$$u^{sc}(r, \theta) \sim D^u(\theta, \theta^{in}) \frac{e^{i(kr - \pi/4)}}{(2\pi kr)^{1/2}}. \quad (6.1)$$

Now we keep the geometry and the incident wave the same, but alter the boundary conditions on one strip; the solution to this new problem is  $w(x, y)$ . We use  $u$  and  $w$

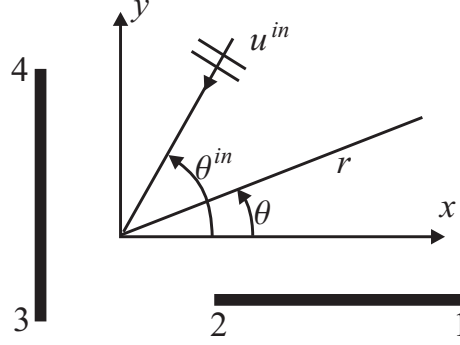


Fig. 7 Geometry of the problem.

for the fields in each case to keep the two problems notationally distinct. We keep the conditions on the segment 1–2 as Dirichlet, but change those on the segment 3–4 to be Neumann so that

$$\frac{\partial w}{\partial x} = 0 \quad (6.2)$$

on its surface. Again one can define a directivity for this new problem:

$$w^{sc}(r, \theta) \sim D^w(\theta, \theta^{in}) \frac{e^{i(kr - \pi/4)}}{(2\pi kr)^{1/2}}.$$

One can write down the local edge asymptotics of the first ( $u$ ) and the second ( $w$ ) problems. For the first one for all the edges  $n = 1 \dots 4$  the asymptotics are

$$u(\rho_n, \phi_n) = K_n^u(\theta^{in}) \rho_n^{1/2} \sin(\phi_n/2) + \text{regular terms} + O(\rho_n^{3/2}). \quad (6.3)$$

For the second problem at the edges  $n = 1, 2$  the asymptotics are

$$w(\rho_n, \phi_n) = K_n^w(\theta^{in}) \rho_n^{1/2} \sin(\phi_n/2) + \text{regular terms} + O(\rho_n^{3/2}). \quad (6.4)$$

In (6.3) and (6.4) the regular terms denote an analytic function having asymptotics  $O(\rho_n)$  in the vicinity of the vertex. At  $n = 3, 4$  the form of  $w_n$  changes to account for the Neumann conditions

$$w(\rho_n, \phi_n) = K_n^w(\theta^{in}) \rho_n^{1/2} \cos(\phi_n/2) + \text{regular terms} + O(\rho_n^{3/2}). \quad (6.5)$$

Here the regular terms are of  $O(1)$ . The local cylindrical coordinates  $(\rho_n, \phi_n)$  are shown in Fig. 8, and  $K_n^u, K_n^w$  are coefficients that we will identify later.

## 6.2 Edge Green's functions

We need edge Green's functions for both problems:  $\hat{u}_m, \hat{w}_m, m = 1 \dots 4$  that obey the Helmholtz equation, and the same boundary conditions as  $u$  and  $w$  respectively. They must also obey the radiation condition at infinity.

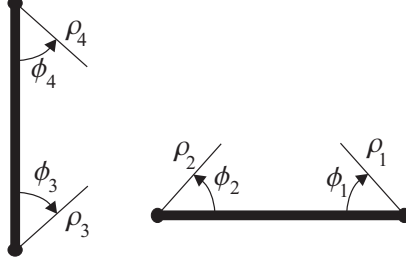


**Fig. 8** Local cylindrical coordinates

In this example we will not need edge Green's functions that have highly oversingular behaviour at the vicinities of the corresponding edges. The edge Green's functions of first order will suffice. These functions are uniquely specified by the over-Meixner terms in the following local expansions

$$\begin{aligned}
 \hat{u}_m(\rho_n, \phi_n) &= \delta_{mn} \rho_n^{-1/2} \sin(\phi_n/2) + \text{Meixner terms} , & n = 1 \dots 4, \\
 \hat{w}_m(\rho_n, \phi_n) &= \delta_{mn} \rho_n^{-1/2} \sin(\phi_n/2) + \text{Meixner terms} , & n = 1, 2, \\
 \hat{w}_m(\rho_n, \phi_n) &= \delta_{mn} \rho_n^{-1/2} \cos(\phi_n/2) + \text{Meixner terms} . & n = 3, 4.
 \end{aligned} \tag{6.6}$$

By analogy with (6.1) we define the directivities for the edge Green's functions as  $\hat{D}_m^u$  and  $\hat{D}_m^w$ , and these directivities are connected with the coefficients  $K_m^u, K_m^w$  from (6.3), (6.4), (6.5). This is analogous to the argument leading to (2.15) and one applies Green's theorem either to the pair of solutions  $u, \hat{u}_m$  or to the pair  $w, \hat{w}_m$  obtaining the formulae

$$K_m^u = -\frac{2i}{\pi} \hat{D}_m^u(\theta^{in}), \quad K_m^w = -\frac{2i}{\pi} \hat{D}_m^w(\theta^{in}) \tag{6.7}$$

relating the near fields of the physical problem to the far-fields of the edge Green's function problems.

### 6.3 The embedding formula

First, we note the following useful properties of derivatives of the physical problems. The function  $\partial u(x, y)/\partial x$  is also a solution of Helmholtz's equation. This function obeys Dirichlet conditions on the faces of the segment 1–2, and Neumann conditions on the faces of the segment 3–4. The last fact becomes clear after noting that

$$\frac{\partial^2 u}{\partial x^2} = -\left(\frac{\partial^2}{\partial y^2} + k^2\right) u \equiv 0$$

on the faces of the segment 3–4. Similarly, the function  $\partial w/\partial x$  obeys the Helmholtz equation and boundary conditions of the Dirichlet type on the faces of the segments 1–2 and 3–4. Let us now consider the combinations

$$v_1 = \frac{\partial u}{\partial x} + ik \cos \theta^{in} w, \quad v_2 = \frac{\partial w}{\partial x} + ik \cos \theta^{in} u.$$

i.e. coupled differential operators. The combinations  $v_1$  and  $v_2$  satisfy the boundary conditions for the second ( $w$ ) and first ( $u$ ) problems, respectively. Both combinations also obey the radiation condition since the incident wave is nullified in both cases. Next consider the edge asymptotics of  $v_1$  and  $v_2$ . Direct calculations show that to leading order

$$\begin{aligned} v_1(\rho_1, \phi_1) &= \frac{K_1^u}{2} \rho_1^{-1/2} \sin(\phi_1/2), & v_1(\rho_2, \phi_2) &= -\frac{K_2^u}{2} \rho_2^{-1/2} \sin(\phi_2/2) \\ v_1(\rho_3, \phi_3) &= \frac{K_3^u}{2} \rho_3^{-1/2} \cos(\phi_3/2), & v_1(\rho_4, \phi_4) &= \frac{K_4^u}{2} \rho_4^{-1/2} \cos(\phi_4/2) \\ v_2(\rho_1, \phi_1) &= \frac{K_1^w}{2} \rho_1^{-1/2} \sin(\phi_1/2), & v_2(\rho_2, \phi_2) &= -\frac{K_2^w}{2} \rho_2^{-1/2} \sin(\phi_2/2) \\ v_2(\rho_3, \phi_3) &= -\frac{K_3^w}{2} \rho_3^{-1/2} \cos(\phi_3/2), & v_2(\rho_4, \phi_4) &= -\frac{K_4^w}{2} \rho_4^{-1/2} \cos(\phi_4/2). \end{aligned}$$

After applying uniqueness, the combinations

$$\bar{v}_1 = v_1 - \frac{1}{2}(K_1^u \hat{w}_1 - K_2^u \hat{w}_2 + K_3^u \hat{w}_3 + K_4^u \hat{w}_4), \quad \bar{v}_2 = v_2 - \frac{1}{2}(K_1^w \hat{u}_1 - K_2^w \hat{u}_2 - K_3^w \hat{u}_3 - K_4^w \hat{u}_4)$$

are seen to be

$$\bar{v}_1 \equiv 0, \quad \bar{v}_2 \equiv 0. \quad (6.8)$$

Finally, comparing the directivities of the terms of (6.8) and using (6.7), we derive two relations

$$\begin{aligned} -\pi k(\cos \theta D^u(\theta, \theta^{in}) + \cos \theta^{in} D^w(\theta, \theta^{in})) &= \\ \hat{D}_1^u(\theta^{in}) \hat{D}_1^w(\theta) - \hat{D}_2^u(\theta^{in}) \hat{D}_2^w(\theta) + \hat{D}_3^u(\theta^{in}) \hat{D}_3^w(\theta) + \hat{D}_4^u(\theta^{in}) \hat{D}_4^w(\theta), & (6.9) \end{aligned}$$

$$\begin{aligned} -\pi k(\cos \theta^{in} D^u(\theta, \theta^{in}) + \cos \theta D^w(\theta, \theta^{in})) &= \\ \hat{D}_1^u(\theta^{in}) \hat{D}_1^w(\theta) - \hat{D}_2^u(\theta^{in}) \hat{D}_2^w(\theta) - \hat{D}_3^u(\theta^{in}) \hat{D}_3^w(\theta) - \hat{D}_4^u(\theta^{in}) \hat{D}_4^w(\theta). & (6.10) \end{aligned}$$

These are then solved to obtain an embedding formula for  $D^u(\theta, \theta^{in})$ :

$$D^u(\theta, \theta^{in}) = \frac{\sum_{n=1}^4 (\alpha_n \cos \theta \hat{D}_n^u(\theta^{in}) \hat{D}_n^w(\theta) + \beta_n \cos \theta^{in} \hat{D}_n^u(\theta) \hat{D}_n^w(\theta^{in}))}{\pi k(\cos^2 \theta - \cos^2 \theta^{in})} \quad (6.11)$$

$$\alpha_1 = \alpha_3 = \alpha_4 = -1, \quad \alpha_2 = 1,$$

$$\beta_1 = 1, \quad \beta_2 = \beta_3 = \beta_4 = -1.$$

An embedding formula for  $D^w(\theta, \theta^{in})$  can be deduced in a similar fashion. Thus the directivity for one problem is found in terms of the edge Green's functions of both. The point of this example is that the edge Green's functions, once found for some geometry, can then be stored and used to provide, in part, directivities even when the boundary conditions change and this can provide a useful cross-verification.



## 7. Concluding remarks

The present article extends embedding theory in a couple of distinct directions. First, it is now clear that cracks inclined to each other, or to a boundary, can be incorporated within the ideological scheme. Second, the application of coupled operators is worth knowing, and applying, to further extend the utility of any edge Green's functions that have been found. This is akin to Babinet's principle which allows one to manipulate and re-use solutions of one diffraction problem for another. In both of these directions many implementations can be made, and existing software utilised, to reduce computational times. Embedding formulae are also interesting as it is intriguing that such non-trivial connections exist between different scattering problems.

**Acknowledgments:** The authors gratefully acknowledge the support of the EPSRC through grant number EP/D045576/1. One of us, RVC, thanks the Departments of Mathematics at the Universities of Alberta and British Columbia for their hospitality during the writing of this article. AVS thanks the Russian Foundation for Basic Research for their support within grant number 07-02-00803.

## References

1. C. M. Linton, P. McIver, Handbook of mathematical techniques for wave/structure interactions, Chapman-Hall CRC Press, 2001.
2. D. G. Crighton, A. P. Dowling, J. E. Ffowcs-Williams, M. A. Heckl, F. G. Leppington, Modern Methods in Analytical Acoustics, Springer-Verlag, 1992.
3. D. S. Jones, Acoustic and electromagnetic waves, Oxford University Press, 1986.
4. J. D. Achenbach, A. K. Gautesen, H. McMaken, Ray methods for waves in elastic solids, Pitman, 1982.
5. M. H. Williams, Diffraction by a finite strip, Q. Jl. Mech. Appl. Math. 35 (1982) 103–124.
6. A. K. Gautesen, On the Green's function for acoustical diffraction by a strip, J. Acoust. Soc. Am. 74 (1983) 600–604.
7. P. A. Martin, G. R. Wickham, Diffraction of elastic waves by a penny-shaped crack: analytical and numerical results, Proc. R. Soc. Lond. A 390 (1983) 91–129.
8. N. R. T. Biggs, D. Porter, D. S. G. Stirling, Wave diffraction through a perforated breakwater, Q. Jl. Mech. appl. Math. 53 (2000) 375–391.
9. N. R. T. Biggs, D. Porter, Wave diffraction through a perforated barrier of non-zero thickness, Q. Jl. Mech. appl. Math. 54 (2001) 523–547.
10. N. R. T. Biggs, D. Porter, Wave scattering by a perforated duct, Q. Jl. Mech. Appl. Math. 55 (2002) 249–272.
11. N. R. T. Biggs, D. Porter, Wave scattering by an array of perforated breakwaters, IMA J. Appl. Math. 70 (2005) 908–936.
12. D. Porter, The solution of integral equations with difference kernels, J. Int. Eqns. Appl. 3 (1991) 429–454.
13. R. V. Craster, A. V. Shanin, E. M. Doubravsky, Embedding formulae in diffraction theory, Proc. R. Soc. Lond. A 459 (2003) 2475–2496.
14. A. V. Shanin, Modified Smyshlyaev's formulae for the problem of diffraction of a plane wave by an ideal quarter plane, Wave Motion 41 (2005) 79–93.
15. A. V. Shanin, Coordinate equations for a problem on a sphere with a cut associated with diffraction by an ideal quarter plane, Q. J. Mech. Appl. Math. 58 (2005) 289–308.

16. R. V. Craster, A. N. Shanin, Embedding formulae for diffraction by rational wedge and angular geometries, *Proc. R. Soc. Lond. A* 461 (2005) 2227–2242.
17. N. R. T. Biggs, A new family of embedding formulae for diffraction by wedges and polygons, *Wave Motion* 43 (2006) 517–528.
18. B. Noble, *Methods based on the Wiener-Hopf technique*, Pergamon Press, 1958.
19. J. B. Keller, The geometric theory of diffraction, *J. Opt. Soc. Amer.* 52 (1962) 116–130.
20. M. Abramowitz, I. A. Stegun, *Handbook of Mathematical Functions*, Dover, New York, NY, 1969.
21. F. L. Neerhoff, J. H. M. T. Van der Hijden, Diffraction of elastic waves by a sub-surface crack (anti-plane motion), *Journal of Sound and Vibration* 93 (1984) 523–536.